The Thesis Committee for Sonya Maria Veron certifies that this is the approved version of the following thesis:

Defining the mechanisms of uncoupling protein 3-induced thermogenesis and metabolism in brown adipose tissue

Approved Supervising Committee:

Supervisor: _____
Edward M. Mills

_____
Andrea C. Gore

Defining the mechanisms of uncoupling protein 3-induced thermogenesis and metabolism in brown adipose tissue

by

Sonya Maria Veron, B.S.

Thesis

Presented to the Faculty of the Graduate School

of The University of Texas at Austin

in Partial Fulfillment

of the Requirements

for the Degree of

Master of Science in Pharmaceutical Sciences

The University of Texas at Austin

December 2014

Acknowledgments

There are no words that can adequately express the gratitude I feel towards my mentor Ted. He has been a guide to me throughout the entirety of this intense process, always supportive and honest in his criticisms and compliments. I entered graduate school with no experience in cell and molecular biology research, and was accepted into Ted's lab with much support and encouragement. Here I gained a thorough understanding of the techniques and strategies used to test pharmacological and biological hypothesis and grew into an independent researcher. Throughout my time in graduate school Ted taught me much about science, life, and more, and he has contributed positively to my life and development as an adult.

I would like to thank the entire Department of Pharmacology/Toxicology for allowing me to speak freely during classes and ask any question that came to mind. The wonderful and friendly educational environment made learning so exciting and made the content easier to understand. Furthermore, the faculty in the department has always been friendly and gracious towards me, and I wish everyone the best with their future pursuits in science.

Lastly I would like to thank my husband, Steve, and my family. They have been my strongest source of support throughout my time in Austin. My family has always stressed the importance of bettering oneself through an excellent education, strong work ethic, and compassion towards humanity. I knew I could accomplish what I set my mind to with their love and support.

Defining the mechanisms of uncoupling protein 3-induced thermogenesis and metabolism in brown adipose tissue

Sonya Maria Veron, M.S.P.S

The University of Texas at Austin, 2014

Supervisor: Edward M. Mills

Uncoupling proteins (UCPs) constitute a highly conserved subset of mitochondrial solute carriers. Discovered in small rodents in the early 1970's, UCPs and their homologs have since been found in nematodes, plants, birds, and, most recently, in significant depots within humans (Krauss *et al.* 2005*,* Van marken Lichtenbelt 2009). Following activation by long chain fatty acids (LCFA, *e.g.* oleic acid) and reactive oxygen species (ROS, *e.g.* 4-hydroxynonenal (4HNE)), UCPs form a proton channel within the inner mitochondrial membrane and permit the influx of hydrogen ions from the inter membrane space into the mitochondrial matrix. UCPs effectively uncouple oxidative phosphorylation (OX-PHOS) from ATP generation, resulting in increasing oxygen consumption and dissipating the chemical energy in the form of heat. Found primarily in brown adipose tissue (BAT) of small hibernating mammals, the canonical role of uncoupling protein 1 (UCP1) in mammalian adaptive thermogenesis has been thoroughly studied. However, UCP1 is not the only member of the uncoupling family found within BAT. Also playing a key role in this tissue is uncoupling protein 3 (UCP3), which is a close homolog

to UCP1. However, in spite of the fact that UCP3 shares more than 50% amino acid homology and tissue localization with UCP1, the true function UCP3 is very poorly elucidated. Part of the difficulty in determining this function lies in the expression levels of the UCP3 protein, which are hundreds of folds less than UCP1 in this tissue. In addition, their homologous structure makes teasing apart UCP3-specific phenomena from UCP1-mediated mechanisms very difficult using conventional techniques in cell and molecular biology.

While UCP1 is almost exclusively found in BAT, UCP3 is expressed primarily in skeletal muscle (SKM), which lacks UCP1 completely (Krauss *et al.* 2005). Because UCP3 is so enriched in SKM, many studies have focused on its role in that tissue and have then tried to transpose these functions into BAT. As a result, UCP3 has been implicated in facilitating numerous biological processes, including non-adaptive facultative thermogenesis, affecting SKM oxidative capacity by modulating LCFA export, and ameliorating elevated levels of ROS-mediated stress within the tissue via glutathionine (GSH) interacting moieties. Ultimately, however, little consensus exists on the function of UCP3 within SKM, and subsequently, even less is known about its purpose in BAT.

Previous data has shown that murine UCP1 has the capacity to bind to itself and form homo-tetramers when expressed *in vitro* in recombinant *E. coli* (Hoang T. *et al.* 2013). Here we show that UCP1 interacts with UCP3 in BAT *in vivo*, supporting Hoang's research above by showing that UCP1 has the capacity to not only homodimerize but potentially oligomerize with other UCP homologs. While many groups using UCP3-null mice have reported no gross changes in physiologic responses, data previously published in the lab showed that mice lacking UCP3 were protected from potentially fatal hyperthermic effects when administered sympathomimetic agents such as 3,4-Methylenedioxymethamphetamine (MDMA), methamphetamine (METH),

lipopolysaccharide (LPS), or norepinephrine (NE) (Mills *et al.* 2003, Kenaston *et al.* 2010). This implies that UCP3 plays an intimate role in sympathetic nervous system (SNS) mediated thermogenesis. Based upon the foregoing, the primary goal of the research discussed in this thesis was to elucidate the functions of UCP3 within BAT.

In this study, we recapitulated results seen by other students in this lab: that global UCP3-null mice do indeed exhibit a blunted thermogenic response when treated with sympathomimetic agonists. In addition, despite the near-ubiquitous expression of UCP2 throughout the mammalian organism, this UCP is not involved in SNS-mediated thermogenesis (Arsenijevic *et al.* 2000). Our data shows that UCP3 is vital to the catecholamine-mediated thermogenic responses following sympathomimetic drug administration. When challenged by METH, UCP3-null mice were able to respond, albeit with a blunted increase in body temperature. Furthermore, when challenged by NE, a key neurotransmitter involved in mediating the responses initiated by the SNS following METH exposure, UCP3-null mice were able to mount half the hyperthermic response seen in WT littermates. However, UCP1/UCP3 double-null animals exhibited an almost four-fold hypothermic effect compared to WT littermates when challenged with NE. In addition, UCP1/UCP3 double-null mice were unable to restore body temperatures back to baseline values, an effect seen in all the other genotypes. This implies that UCP3 plays an important role in restoring body temperatures to physiological norms. Therefore, while the mechanism underlying the decreased responsiveness to NE remains unclear, it is clear that whether localized to SKM or BAT, UCP3 is a major player in the mammalian response to SNS-mediated thermogenesis and global thermoregulation.

Table of Contents

List of Figures

List of Abbreviations

4-HNE	4-Hydroxynonenal
ANT	Adenine nucleotide translocase
ATP	Adenosine triphosphate
BAT	Brown adipose tissue
BMR	Basal metabolic rate
β-ox	Beta oxidation
BSA	Bovine serum albumin
PGC1α	Peroxisome proliferator-activated receptor gamma coactivator 1-alpha
CO_2	Carbon dioxide
DCI	Δ3,5Δ2,4dienoyl-CoA isomerase
EDTA	2,2‟,2”,2”‟-(ethane-1,2-diyldinitrilo) tetraacetic acid
EGTA	Ethylene glycol tetraacetic acid
ETC	Electron transport chain
FA	Fatty acid
FAO	Fatty acid oxidation
FBS	Fetal bovine serum
FCCP	Trifluorocarbonylcyanide Phenylhydrazone
FFA	Free fatty acid
GSH	Glutathione
H+	Proton
HBSS	Hank's buffered salt solution
HEPES	4-(2-hydroxyethyl)-1-piperazineethanesulfonic acid
IGF-1	Insulin-like growth factor 1
LCFA	Long Chain Fatty Acids
METH	Methamphetamine
MDMA	3,4-Methylenedioxymethamphetamine
MH	Malignant hyperthermia
mRNA	Messenger RNA
NaCl	Sodium chloride

NaOH	Sodium hydroxide
NE	Norepinephrine
OX-PHOS	Oxidative Phosphorylation
PAGE	Polyacrylamide gel electrophoresis
PCR	Polymerase chain reaction
PGE_2	Prostaglandin E2
PM	Plasma Membrane
PMSF	Phenylmethylsulfonyl fluoride
PPAR	Peroxisome proliferator-activated receptor
RIPA	Radioimmune precipitation assay buffer
RNA	Ribonucleic acid
SDS	Sodium dodecyl sulfate
SNS	Sympathetic nervous system
SKM	Skeletal muscle
T2DM	Type II diabetes mellitus, insulin-dependent diabetes mellitus
TCA	Tricarboxylic acid Cycle
Tris-HCl	Tris(hydroxymethyl)aminomethane hydrochloride
UCP	Uncoupling protein
V/V	Volume / volume
WAT	White adipose tissue

Chapter 1 – Introduction

The eukaryotic mitochondria is called the "powerhouse" of the cell. However, this moniker is a gross oversimplification of the diverse functions of the most important, if not the most functionally diverse, organelle. Mitochondria are responsible for a tremendous host of intercellular processes: from the synthesis of all the Citric acid cycle (TCA) intermediates, to beta-oxidation (β-ox), calcium signaling, ROS damage mediation, apoptosis, and perhaps the most famous – OX-PHOS coupled with adenosine triphosphate (ATP) generation. Furthermore, mammalian mitochondria are home to a family of solute carriers responsible for mediating the majority of non-shivering thermogenesis seen in mammals –UCPs. Twenty-first century science transformed a plethora of previously terminal conditions such as Acquired Immune Deficiency Syndrome (AIDS) and many cancers into manageable illnesses – kept in check by one pill a day. However, despite great advances in biology, mitochondrial related illnesses such as Huntington's disease, Alzheimer's, and rapid dementia still plague millions around the world.

Current research suggests that states of over nutrition, where caloric consumption exceeds expenditure, drive mitochondrial dysregulation of the electron transport chain (ETC). Caloric excess continuously feeds substrate into the TCA cycle without providing an outlet for the dissipation of the excess ATP. This results in increased flux across the ETC creating a bottle-neck effect at ATP synthase but stalling the electron handling machinery, leading to electron slippage off of the ETC and into the surrounding mitochondrial matrix. Here freed electrons can react with molecular oxygen generating the free radical superoxide. If this ROS is not quenched by ROS scavenging molecules such as GSH it will continue to harvest electrons from other mitochondrial substrates leading to the generation of even more deleterious ROS species, such as the peroxidated lipid 4HNE.

These and other ROS cause damage to the sensitive neurons making up the basal ganglia and other cerebral regions leading to the onset of debilitating neurological conditions. However, UCPs act as a safety valve throughout OX-PHOS, and have the capacity to alleviate the stress excess electrons cause to the ETC. Found within the mitochondrial matrix plasma membrane, these protonophores extrude protons from the intermembrane space into the matrix, decreasing the electrochemical gradient, and act as a safety valve on the ETC. By preventing this undue burden UCPs indirectly decrease ROS, prevent the cell from having an excess of ATP, burn excess energy, and allow the TCA cycle as well as OX-PHOS to proceed unhindered.

Recently, exciting research has shown the existence of functioning depots of BAT in active, lean, adult males, sparking much resurgence in the interest in this group of protonophores (Van marken Lichtenbelt *et al*, 2009). With obesity affecting a staggering 30% of the United States adult population, the ability to dissipate excess caloric energy by activating BAT depots has become a very attractive therapeutic option, especially as pharmacologic intervention has proven grossly ineffective in combatting this disorder. By targeting UCPs, researchers have the ability to ameliorate these devastating illnesses while increasing the quality of life for millions around the world.

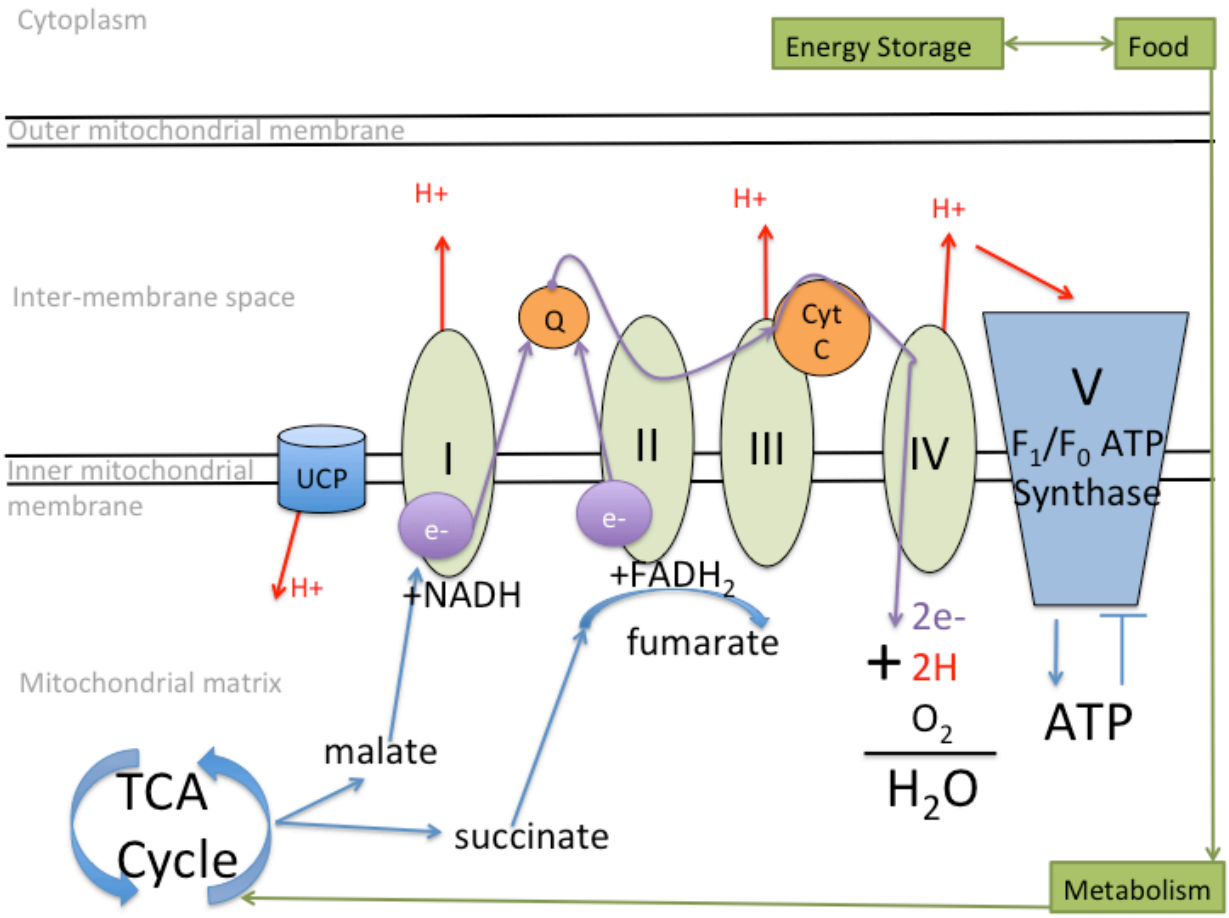

Figure 1. Oxidative phosphorylation and ATP generation After food is consumed, it may be stored for later use or directly transported into the mitochondria for metabolism. Once inside the mitochondria, metabolites enter the Citric Acid cycle and are oxidized to drive the extrusion of protons to the intermembrane space. Along with NADH and $FADH_2$ as cofactors, an electron is shuttled from these complexes to coenzyme Q and then to complex III. Electrons are passed via heme groups within shuttling protein, cytochrome C, to complex IV where they are combined with 2 protons and molecular oxygen to catalyze the formation of water. Throughout this entire process, complex I, III, and IV, release protons into the intermembrane space, and UCPs shuttle protons back into the mitochondrial matrix. Protons from the intermembrane space generate an electrochemical gradient and power F1/F0 ATP synthase allowing for the formation of ATP from ADP and inorganic phosphate.

1.1 Metabolism

Metabolism is the biological application of the first law of thermodynamics. It is the summation of every energetically consuming and generating reaction in an organism. Yet, despite this simplistic statement, an organism rarely functions at levels where most of its nutrients are immediately consumed. Despite great advances in research methodology, quantifying metabolism is still very difficult. Most studies typically measure basal metabolic rate (BMR), the metabolism of an organism at rest at thermoneutral temperatures (Argyropoulos 2002). With these variables held constant, BMR is predominantly a reflection of the mass and metabolic capacity of internal organs, and is usually directly proportional to the complexity and size of the organism. (Mckechnie 2008) However, mammalian metabolism is not a static value and is actively under the influence of a confluence of factors such as nutritional status, age, sex, external temperature, and thyroid hormone activity (Silva 2001).

The most comprehensive methods to assess whole-body metabolism involve utilizing plethysmography chambers. These chambers are specially constructed to establish an animal's metabolic profile by collecting and analyzing urine, feces, as well as precisely monitoring changes in CO_2/O_2 gas volume and pressure to give a precise measurement for lung capacity (Criée *et al.* 2011). In addition, complementary techniques, such as dual energy x-ray absorptiometry, are often employed simultaneously to further assess the bone mineral density, fat and lean body mass, as well as water content of the animal. However, these methods cost thousands of dollars to implement, making them prohibitively expensive for small studies. More conventional methodology utilizes aerobic respiration to measure metabolism. In these systems, an organism is placed into a sealed chamber enriched with CO_2. Then, expired CO_2 and inspired O_2 is collected, analyzed, and translated into a rate of gas exchange. Unlike plethysmography

chambers, conventional respirometry utilizes a spectrophotometer-like construct where the change in the infrared spectrum following CO_2 absorption can be plotted against the change in CO_2 concentration using a photomultiplier tube and Lambert's law (Tøien, 2013).

Additional methods of metabolic assessment utilize external thermogenic challenges, as a proxy metabolic measurement. Using an implanted temperature probe, changes in intraperitoneal body temperature are monitored following subcutaneous administration of thermogenic agonist such as NE, a SNS agonist which is known to cause a rise in core body (Melin *et al.* 1988). These changes are subtracted from a baseline body temperature and this magnitude is used to indicate the metabolic capacity to respond to the thermogenic challenge. This eliminates the need for costly chambers and gas sensors. In addition, these types of studies provide researchers with a more mechanistic view of SNS-mediated metabolism rather than a broad calculation of an organisms' basal metabolic rate which fluctuates greatly.

1.2 Thermoregulation

Thermoregulation and thermogenesis are two faces on the same metabolic coin. These processes are vital to developing life and differ greatly depending on the organism. Reptiles, frogs, crickets, and other ectotherms, organisms whose body temperature and metabolic rate depend greatly on their external temperature, use behavioral methods of thermogenesis, such as basking in the sun on a hot rock, to maintain their body temperatures. Ectotherms rely heavily on physiological methods of heat transfer to stay warm in fluctuating temperatures. For example, fish have evolved sophisticated countercurrent system of thermoregulation in which arteries and veins run very closely and counterparallel to one another. Heat is able to

diffuse down its temperature gradient to nearby blood vessels, facilitating the flow of heat around the body (Malte *et al* 2007). If the external environment is too warm, frogs will increase mucous secretion to decrease body temperature via evaporation. Conversely, if temperatures are too cold, many ectotherms will enter a state of torpor characterized by a tremendous drop in body temperature and metabolism. Ectotherms are essentially "frozen" in this state unable to move, reproduce, feed, or digest food for periods that can last as long as eight months (Hochaka *et al.* 1985). During this period the majority of fuel substrates comes from lipid stores but other energetic substrates, such as molecular oxygen, can be limiting if an organism spends most of its life submerged in water, like turtles. Yet, torpor ensures that oxygen and fuel conservation occurs while keeping anaerobic end products, such as lactate, at low levels, and prevents systemic acidosis due to CO_2 accumulation. Ectotherms will actively seek areas of optimal temperatures to maintain homeostasis. As a consequence, their lifespan, body size, metabolisms, and energetic capacity are highly limited by their environment.

In contrast, mammals, or endotherms, have the ability to live in almost any environment due to their internal mechanisms of thermoregulation. Unlike ectotherms, endotherms have an internal set temperature that does not fluctuate with environmental changes. Briefly, receptors in the skin feel changes in the ambient environment and send afferent signals to the anterior hypothalamus where signals are integrated with information received from the body's baroreceptors and osmoreceptors. Body temperature can be manipulated further by the presence of prostaglandins, inflammatory cytokines, as well as SNS tone (Netea *et al.* 2000). If the environment is too cold, the brain acts in concert with other organs and tissues to increase body heat transmission by activating BAT, inducing vasodilation, and shivering.

In addition, animals may increase body heat transmission by participating in a variety of non-exercise behaviors such as nesting, nursing, cuddling with littermates, or alternating their body postures (Hochaka *et al* 1985).

In addition to an internal set point, endotherms have evolved a number of unique advantages, such as fur and brown adipose tissue (BAT), to maintain a constant internal temperature, a process known as thermogenesis. Thermogenesis can be broken down into two primary categories: obligatory and facultative. Obligatory thermogenesis encompasses the metabolic energy necessary to run all of the biological processes within the organism: food absorption, digestion, and metabolism, movement, which is both voluntary and involuntary, as well as diet-induced thermogenesis (Himms-hagen 1995). Facultative thermogenesis can be rapidly initiated in situations which require additional energy to maintain homeostasis such as shivering, exercise, exposure to prolonged periods of cold, and is associated with the activation of SKM and BAT (Silva 2001). This increases blood flow around the body and initiates lipolysis, stimulating the activation of UCP3, the primary UCP found within SKM concurrently with the UCPs found in BAT. Thus, endotherms possess very high metabolic rates despite tremendous variation in body sizes and organismal complexities. These mechanisms facilitate their survival in varying environmental conditions found on the Earth.

1.3 Dysregulation of Thermogenesis: From Fevers to Hyperthermia

One of the more understood thermogenic phenomena are fevers. A fever is defined by an elevation in core body temperature by 1-4°C (Saper *et al.* 1994). This elevation in temperature is common during bacterial infections and is thought to provide adaptive immunity to its host by increasing the efficacy of neutrophil and macrophage attacks, as well as impeding the replicative potential of the invading pathogen. Fevers are initiated when endogenous pyrogens cross the blood brain barrier and enter the hypothalamus. There they initiate a cascade of inflammatory signaling which leads to the production of prostaglandin E2 (PGE_2) (Netea *et al.* 2000). Together with second messenger cyclic adenosine monophosphate (cAMP), PGE_2 elevate body temperature and initiate the physiologic symptoms associated with fevers (Dinarello *et al* 1984).

At one end of the spectrum low-grade fevers offer the host a range of physiological benefits. However, if the body temperature becomes too high heat strokes or malignant hyperthermia (MH) can result. Heat stroke occurs when body temperature is above 40°C. It is usually a direct result of environmental factors combined with the inability to dissipate heat efficiently due to infirmity, old age, or other factors (Glazer 2005). MH is a pharmacogenetic disorder that occurs in patients with an autosomal dominant mutation in their SKM ryanodine receptors. This results in a "leaky" ryanodine receptor that depletes the sarcoplastmic reticulum of its calcium stores, uncoupling calcium flux from muscular contractions in a mechanism similar to how UCPs uncouple OX-PHOS from ATP synthesis (Ferreiro *et al.* 2002, Ali *et al* 2003, Chelu *et al*. 2006). This futile cycle can be recapitulated in some patients by the administration of halogenated anesthetics like isoflurane. Depending on the severity, patients with MH can present with a variety of symptoms ranging from anxiety, muscular spasms, tachycardia, and even renal failure. If body temperatures are not rapidly decreased, over 50% of all MH patients will succumb to

death as a result of intravascular coagulation, rhabdomyolysis leading to renal failure, or cerebral edema (Jurkat-rott *et al*. 2000).

An acute, non-genetic form of MH can occur in individuals who consume MDMA. MDMA, nicknamed "ecstasy" is a very popular club drug around the world. Upon oral administration, once MDMA has crossed the blood-brain barrier it triggers a large release of dopamine, serotonin, and NE onto the CNS as well as the periphery. The activation of lipolysis by circulating NE results in the liberation of FFA and subsequent activation of SKM UCP3. This, in conjunction with thyroid hormone levels is postulated to mediate the hyperthermic response seen with recreational MDMA use (Rusyniak *et al.* 2005). Furthermore, Sprague *et al.* prevented and attenuated MDMA-induced MH by treating patients with α_1 and the $\beta_{1,2,3}$ adrenergic receptor antagonist carvedilol, demonstrating that MDMA-induced MH is indirectly mediated by both the α_1 and the β_3 adrenoreceptors. (Sprague *et al.* 2005).

1.4 Brown Adipose Tissue

Brown adipose tissue (BAT) is a highly metabolic tissue found in the interscapular, perirenal, axillary, and paravertebral areas of many hibernating mammals including mice, rats, and hamsters (Casteilla *et al.* 2008). In small rodents BAT depots continue to develop and grow until the animal is sexually mature. However, BAT expression in humans differs greatly from rodents where it localizes primarily on the ventral side of the body between the shoulder blades and gradually atrophies as the infant develops into adulthood. Recent studies utilizing fluorescent tracers have shown that BAT is present in active, lean males with expression directly relating to levels of exercise and activity (Van marken lichtenbelt *et al.* 2009). This discovery has sparked

great re-interest in the metabolic capacity of this tissue. After infancy, BAT localization shifts to the dorsal side of the body where it is found mostly around the sternum and the interclavicle areas (Van marken lichtenbelt 2009). Here, in conjunction with white adipose tissue (WAT) and thyroid hormone, BAT is intimately involved in body temperature regulation of the abdomen and internal organs.

Containing an abundance of UCP1, BAT is responsible for maintaining body temperature, especially during periods of intense cold. This differs starkly from WAT – which functions mainly as an energy storage organ and endocrine regulator releasing adipokines such as leptin, ghrelin, and adiponectin during various states of organismal nutrition. However, BAT adipocytes are distinctly different from WAT adipocytes. BAT adipocytes differ greatly in their morphology, gene signatures, mitochondrial content, enzymatic capacity, and lipid mass. Even before the distinct tissues arise during organogenesis, BAT progenitor stem cells arise from the same population of *Myf5*+ stem cells which will grow to become SKM, not WAT (Seale *et al.* 2008, Martinez-lopez *et al.* 2013). Furthermore, the fully differentiated BAT adipocyte exhibits a multilocular appearance, with its lipid content stored in an abundance of small lipid-dense droplets which surround the nucleus. WAT adipocytes, in contrast, usually contain one large acentric lipid vacuole. Another important distinction between the two tissues is mitochondrial content. BAT is brown because of its enrichment in mitochondria, specifically cytochrome C. This enrichment allows BAT adipocytes to express and store exponentially more fatty acid metabolizing and ROS-quenching enzymes than its WAT counterpart (Forner 2009). In fact, it has been postulated that UCP1 makes up almost 8% of the BAT mitochondrial proteome (Rousset *et al.* 2007). Conversely, WAT is enriched in enzymes responsible for endocrine

communication as well as xenobiotic transformation and matched the gene signature of the liver more closely than that of BAT (Forner *et al.* 2009).

Recently, subcutaneous depots of "beige" cells have been found in WAT (Harms *et al.* 2013). These are WAT adipocytes stimulated to differentiate into BAT-like cells following treatments of cold or β3 adrenergic receptor agonists (Wang *et al*. 2013). While beige adipocytes share BAT adipocyte morphology as well as express low levels of UCP1, UCP3 has not been found in this group of cells. Furthermore, beige cells originate from WAT precursor *Pdgfr-α*+ *Myf5*- progenitor stem cells and are regulated by different transcription factors and pharmacologic agonists than BAT adipocytes. Furthermore, the function of beige cells is under intense scrutiny. While very little is known, some hypothesize that the importance of beige cells lies not in their absolute number, but in the ratio of beige to classical WAT adipocytes, which plays an important role in insulin regulation and glucose homeostasis (Seale *et al*. 2008).

1.5 Mammalian Bioenergetics

Unlike plants which use chloroplasts to harvest their own energy via photosynthesis, most living organisms must obtain energy by the consumption of external fuel sources. This results in the generation of ATP – the ubiquitous energy currency used by all kingdoms of life. Generated within the mitochondria, this energetic substrate allows the mammalian organism to perform a broad array of functions: growth and development, thermoregulation and metabolism, and reproduction. Bioenergetics describes the cyclical flow of chemical energy into and out of an organism (Mckechnie 2008) In mammals, this chemical energy is often lost through the

production of body heat, which, in addition to being energetic waste, serves to protect mammals from the cold and maintain homeostasis. Thus, many researchers use body heat production as an indirect measurement of metabolism and energetic efficiency.

Mitochondria are made up of two separated plasma membranes (PM) forming an inner matrix and an intermembrane space. Situated within the inner mitochondrial membrane is where OX-PHOS occurs (**Figure 1.1**). Briefly, NADH/$FADH_2$ transfer their electrons to complex I and II of the electron transport chain (ETC). From there electrons are transported by Coenzyme Q to complex III where Cytochrome C shuttles electrons to complex IV. As this process occurs, complex I, III, and IV, release protons into the intermembrane space, generating an electrochemical proton gradient and membrane potential across the inner mitochondrial PM. Complex V, or ATP Synthase, then uses this proton gradient to drive the phosphorylation of adenosine di-phosphate into ATP.

Disease pathophysiology occurs when the steady flow of electrons across this chain is disrupted. Electron slippage occurs in states of organismal stress: commonly in overnutrition or extreme exercise, especially between the complexes mediated by electron carrier coenzyme Q and cytochrome C. If freed electrons are not captured by electron scavenging proteins such as N-acetyl cysteine, they will bind to any available matrix protein or mitochondrial substrate leading to the gross accumulation of superoxide and other ROS. This catalyzes a sequence of reactions where by less reactive ROS bind to milieu in the surrounding matrix generating even more deleterious ROS such as peroxidated lipids.

1.6 Uncoupling Proteins

Uncoupling proteins are transmembrane protonophores located within the inner mitochondrial membrane. Like their name suggests, UCPs de-couple the proton electrochemical gradient from ATP synthesis, decreasing the proton flux and membrane potential across the inner mitochondrial membrane. During OX-PHOS, mitochondrial complex I, III, and IV pump protons into the intermembrane space. These protons establish the electrochemical gradient and mitochondrial membrane potential that drives complex V, ATP synthase, to catalyze the formation of ATP from adenosine diphosphate (ADP) and inorganic phosphate back across the matrix membrane. At elevated ratios of ATP to ADP, mitochondrial machinery begins to slow down due to ATP synthase inhibition by excess ADP (Kishikawa *et al.* 2014). UCPs act as a proton channel extruding protons from the intermembrane space back into the matrix, decreasing the mitochondrial membrane potential and electrochemical gradient. Thus, by decreasing the proton availability to ATP synthase, UCPs ensure that mitochondria never possess supramaximal levels of ATP. However, if substrates are continuously fed into the mitochondria while electron flux is slowed this can lead to slippage off of the electron handling machinery, leading to undue ROS burden and mitochondrial damage.

Like many biological processes, UCPs are regulated by both negative and positive feedback loops. When ATP levels become too low, ADP is in abundance. Purine nucleotides like ADP and GDP inhibit UCPs, preventing proton leakage, and allowing for an increase of protons in the intermembrane space, pushing complex V and promoting ATP formation **[cite here]**. Conversely, research has shown that UCPs are activated by long chain fatty acid (LCFA) anions at both the protein and transcriptional level (Mochizuki *et al.* 2006, Fedorenko *et al.* 2012). A diverse group of polyunsaturated FA species bind to and stimulate the activity of peroxisome

proliferator-activated receptor alpha, beta, and gamma (PPARs), transcription factors which have response elements upstream of both UCP1 and UCP3 promoters. At the protein level, the LCFA hydrocarbon tail binds to the cytoplasmic face of UCP1 due to their hydrophobic interactions (Fedorenko *et al.* 2012). Upon protonation, the LCFA anion causes UCP1 to undergo a conformational change, releasing the proton into the mitochondrial matrix. Many FA substrates are capable of binding to UCP1, however research has shown that a higher proton gradient is required to effectively protonate lower pKa FA species. Furthermore, it has been demonstrated that ROS, specifically, 4-HNE and superoxide are potential activators of UCPs, although the mechanism behind such activation is unknown (Echtay *et al.* 2002). This positive regulation of UCPs by ROS is interesting as it suggests that some basal concentration of ROS must exist to trigger the ameliorative actions of UCPs.

At the transcriptional level UCPs are tightly regulated by a large host of transcription factors including PPARs, peroxisome proliferator-activated receptor gamma coactivator 1-alpha (PGC1α) CCAAT enhancer binding proteins (CEBP1α), thyroid hormone, cyclic adenosine monophosphate (cAMP), and retinoic acid, among others, which must be present for strong gene induction (Acín 1999, Solanes 2003 & 2005). Cyclic-AMP is an especially important second messenger because it catalyzes the majority of SNS-mediated uncoupling as a response to cold, fever, or thermogenic drugs. Lastly, some hormones like insulin-like growth factor 1 (IGF-1), induce UCP gene expression. Conversely, glucocorticoids have been shown to reduce UCP gene expression, perhaps due to their transcriptional activity on NE. However, elucidated mechanisms of action remain unclear. (Soumano *et al.* 2000*)*.

1.7 Uncoupling Protein 3

Another protonophore found within the mitochondria of BAT is uncoupling protein 3 (UCP3). Despite being 50% structurally homologous to UCP1, the function of UCP3 in BAT is very poorly understood. This difficulty lies primarily with fact that UCP3 is expressed 500 fold less than UCP1 in BAT, making it very difficult to tease apart UCP3-specific effects. (Harper 2001, 2002). Thus, much of what is known about UCP3 is extrapolated from SKM, where UCP3 predominates, but which has a complete dearth of UCP1. Furthermore, an overall idea of the function of UCP3 is convoluted, with different groups reporting contrasting results.

Studies assessing the function of UCP3 in UCP3-null mice found that there were almost no global physiological changes as a result of UCP3 deletion (Gong 2000, Vidal-puig 2000, Harper 2001, 2002). Body weight, serum analysis including insulin, TG and FFA oxidation were all unchanged from controls. Furthermore, thermogenic responses to exposure to 4°C for 1 hour, 4 hours, and 24 hours was no different from wild-type littermates. Resting oxygen consumption following injection with β3-adrenergic agonist CL314263 resulted in increases of the same magnitude in both genotypes, suggesting a lack of UCP3 involvement in SNS-mediated thermogenesis (Gong 2000). Yet, groups have found that mice subcutaneously administered SNS agonist 3,4-methylenedioxymethamphetamine (MDMA) were protected from the drug's acute hyperthermic effects, indicating that UCP3 does indeed play a role in thermogenesis (Mills *et al.* 2003, Sprague *et al.* 2004, 2007). Furthermore, the majority of the studies performed in UCP3-null mice were conducted in mitochondria from SKM, where UCP3 predominates (Gong 2000, Vidal-puig 2000). These authors are incorrect in making gross extrapolations about the function of UCP3 within BAT from their limited investigation of its function in SKM, a tissue with drastically differing structures, functions, and tissue environment from BAT.

The studies above reported increases in levels of ROS in UCP3-null SKM mitochondria, findings that have been confirmed by other groups (Vidal-puig 2000). These same levels of ROS production could be re-created in WT mice with the treatment of mild uncoupler FCCP, postulating that UCP3 decreases ROS via mild uncoupling mechanisms (Toime *et al.* 2010). Within the mammalian cell, the generation of ROS is very tightly coupled to perturbations within the membrane potential. Thus, it is possible to see pronounced decreases in ROS production with even mild uncoupling by UCP3. However, this phenomenon was argued to be due to increased activity of adenosine nucleotide translocator (ANT) protein and not UCP3 (Bevilacqua 2010). Other studies assessing levels of 4HNE or carbonylated protein production in UCP3-null SKM mitochondrial found no difference among genotypes (Nabben 2011). While other groups found that significant increases in ROS could be mimicked by placing UCP3-null mice on a 2 month high-fat diet, indicative of substrate-specific UCP3 effects. (Nabben 2011).

Yet, other groups believe that the effects of UCP3 on ROS are indirect and not due to classical uncoupling (Maclellan *et al.* 2005). Within the mammalian cell ROS quenching occurs via scavenging molecules such as GSH, and N-acetyl cysteine. Some groups have found reactive cysteine residues on UCP3 that have the capacity to conjugate with GSH (Mailloux *et al.* 2011). They hypothesize that elevated levels of ROS sequester available GSH, triggering the uncoupling capacity of UCP3 in situations of increased ROS burden. Currently, no consensus exists but studies of UCP3 polymorphisms in humans have been linked to metabolic disorders associated with ROS signaling, GSH synthesis, FA oxidation and impaired TG oxidation following overfeeding (Walder 1998, Ukkola 2001, Musa 2012).

1.8 Summary and Concluding Remarks

It is clear that the energetic demands of endotherms are costly yet come with many advantages. The capacity to maintain thermal homeostasis allows mammals to live in a variety of environments, while allowing them to grow to larger sizes and have more complex metabolic and circulatory systems. Specialized tissues like BAT and SKM allow vertebrates to participate in both obligatory thermogenesis as well as activate facultative thermogenesis via shivering whenever additional body warmth is needed. On a molecular level, both of these events are powered by ATP generated within the mitochondria. Consumption of a variety of substrates powers the TCA cycle, generating sugar intermediates, which enter the ETC. These intermediates are donated to the various complexes of the ETC along with reducing cofactors that facilitate the flux of electrons as they move through each complex. As electrons are shuttled down the ETC, complexes I, III, and IV, pump protons into the intermembrane space, generating an electrochemical gradient across the inner mitochondrial membrane. This proton motive force serves to push protons into ATP synthase and facilitate the phosphorylation of ADP and inorganic phosphate to ATP, the energetic currency of the body.

UCPs de-couple the ETC from the generation of the membrane potential, allowing protons to flow back into the mitochondrial matrix. By serving as a "safety-valve" for OX-PHOS, UCPs prevent the accumulation of supramaximal levels of ATP, as well as ensure the steady flow of electrons across the ETC, preventing electron slippage off of handling machinery and the generation of deleterious ROS. Canonical UCP1 is found almost exclusively in BAT where its role and importance in adaptive thermogenesis has been well elucidated. However, the function of its homolog, UCP3, remains poorly understood, and very difficult to decipher. Expressed primarily in SKM, the role of UCP3 in BAT is highly controversial. Part of the difficulty lies in

separating UCP1-mediated effects from UCP3 – functions which could overlap, be complementary, or even synergistic to one another.

The primary goal of this study was to elucidate the effects of UCP3 in BAT. Some groups have found that UCP3 plays an important role in the redox regulation of mitochondria, while others have found that UCP3 in not involved in any aspect of mammalian metabolism (Mailloux *et al.,* Nabben 2011). It is clear that UCP3 is involved in thermogenesis – at least in amphetamine-mediated conditions, suggesting that UCP3 may be activated under special circumstances. (Mills *et al.* 2003). However the true function of UCP3 in BAT is unclear. Much of what is known has been extrapolated from studies assessing the function of UCP3 in SKM, in animals where UCP3 has been globally deleted, or overexpressed to supraphysiological levels. However, UCP3 is the only UCP in SKM, where the redox environment grossly differs from that of BAT mitochondria (Mailloux *et al.* 2012). Thus, it is entirely plausible that the function of UCP3 in BAT differs from that in SKM. While many groups have attempted to explain the mechanisms involved in UCP3-mediated thermogenesis, no universal consensus exists. This study seeks to give more insight into the mechanisms underlying UCP3-mediated thermogenesis as well as to provide mechanistic insight into its interactions with partner proteins in BAT. Data will bolster our understanding of this protonophore and its function within the mammalian mitochondria.

Chapter 2 – Methods and Materials

2.1 Chemicals and Reagents

All chemicals and reagents were received from Sigma Aldrich (St. Louis, MO) unless otherwise stated.

2.2 Animals

C57BL/6 mice were purchased from Jackson Laboratories (Bar Harbor, ME). C57BL6/J UCP3 -/- mice were a gift of Dr. Marc Reitman, formerly of the National Institutes of Health. C57Bl6/J UCP1 -/- mice were gifted by Dr. Leslie Kozak of the Pennington Biomedical Research Institute. UCP1/UCP3 Double-null mice were generated by breeding UCP1-/- mice to UCP3-/- mice and their genotypes verified via polymerase chain reaction (PCR) analysis. Animals were housed in a 12 hour light/dark cycle and fed Prolab RMH 2000 5P06 (5% fat) chow. Mice to be used for experimental procedures were switched to Prolab RMH 2000 9P06 (9% fat) at 6 weeks of age and maintained on this diet for at least 2 weeks. All procedures were approved by the University of Texas Institutional Animal Care and Use Committee.

2.3 PCR

UCP1/UCP3 double-null animal genotypes were confirmed via PCR. Briefly, following weaning, mouse tails were clipped, and DNA isolated using the Wizard Genomic DNA Purification Kit (Promega, Fitchburg, WI) exactly as per the manufacturer's instructions. DNA, positive, and negative controls were then added to individual PCR tubes followed by a master mix containing 10X Advantage® 2 SA PCR Buffer (Clonetech, Mountain View, CA), 10mM dNTPs, and Taq polymerase (Clonetech, Mountain View, CA). For mUCP3, three 20uM unique

primer sequences were added to the master mix: 5'- CTC CAT AGG CAG CAA AGG AAC- '3, 5' - CAA GCA AAA CCA AAT TAA GGG -'3, 5' - CCA CTA TAT GGT TTA CAC AGC -'3. For mUCP1 three separate and unique 20uM primer sets were added to its master mix: 5' - CCT AAT GGT ACT GGA AGC CTG- '3, 5' - CCT ACC CGC TTG CAT TGC TCA- '3, 5' - GGT AGT ATG CAA GAG AGG TGT- '3. Cycling conditions for mUCP3 were as follows: initial denaturing at 94° C for 5 minutes, followed by 35 cycles of 94° C for 1 minute, 60° C for 1 minute, and then annealing at 72° C for 1 minute. Cycling conditions for mUCP1 were identical to mUCP3 with the 35 cycle denaturing temperature at 58° C for 1 minute. Once the PCR was complete, 6X loading dye (30% (v/v) glycerol, 0.25% (w/v) bromophenol blue, 0.25% (w/v) xylene cyanol FF) was added to each sample was separated via DNA-gel electrophoresis on a 1% agarose gel with ethidium bromide (Fischer Scientific, Waltham, MA) and results confirmed using a Biorad UV transiluminator coupled to a camera.

2.4 Tissue Isolation from Mice

Six to eight-week-old male C57BL/6 mice were euthanized via CO_2 asphyxiation, tissues excised and immediately placed into ice-cold CP-1 buffer (100mM KCl, 50mM Tris HCl, 2mM Ethylene glycol tetraacetic acid (EGTA), pH 7.4, supplemented with 200mM Phenylmethylsulfonyl fluoride (PMSF), 1uL/10mL Leupeptin, 1uL/10mL Pepstatin, 7uL/10mL 10,000KIU/mL Aprotonin, 0.42mg/mL NaF, and 200mM Sodium Orthovanadate**)** Remaining WAT was removed and tissues minced into small pieces using laboratory scissors.

2.5 Isolation of Mitochondria

Using a clear glass pestle tissue grinder, samples were completely homogenized and diluted 1:1 with equal volume of CP-1 buffer with 0.2% FA free bovine serum albumin (BSA). Tissues were centrifuged at 600 x g for 5 minutes at 4°C, and the supernatant transferred to a fresh conical. This spin was repeated once more at 700 x g and the supernatant filtered through a 70um cell strainer (Corning, Tewksbury, MA). Tissues were then centrifuged at 7000 x g for 10 minutes at 4°C to isolate mitochondria, the supernatant discarded, and the pellet resuspended in CP-1 buffer without BSA. Mitochondria were washed 3 additional times in ice-cold CP-1 buffer, centrifuged at 7000 x g for 10 minutes at 4°C. Samples were resuspended in 30-60uL of Hirasaka IP Buffer (50mM Tris HCl, 150mM NaCl, 5mM EDTA, 1% Triton X, pH 8, supplemented with 200mM PMSF, 1uL/10mL Leupeptin, 1uL/10mL Pepstatin, 7uL/10mL 10,000KIU/mL Aprotonin, 0.42mg/mL NaF, and 200mM Sodium Orthovanadate**)** or RIPA buffer (50mM Tris-HCl, 1% nonyl phenoxypolyethoxylethanol (NP-40), 0.5% Sodium Deoxycholate, 0.1% SDS, 150mM NaCl, 2mM EDTA, pH 8.0, supplemented 200mM PMSF, 1uL/10mL Leupeptin, 1uL/10mL Pepstatin, 7uL/10mL 10,000KIU/mL Aprotonin, 0.42mg/mL NaF, and 200mM Sodium Orthovanadate).

2.6 Protein Quantification

Protein quantity was determined by via bicinchoninic acid assay (Thermo Scientific Pierce, Rockford, IL) exactly as per the manufacturers' instructions using BSA as a standard. Plates were read in a standard spectrophotometer set to detect 562nm.

2.7 Immunoblotting

To prepare samples for SDS-PAGE following protein quantification, a 5X concentrate of 250mM Tris HCl, 8% SDS, 40% glycerol, 8% β-mercaptoethanol, 0.02% bromophenol blue was added to lysates, boiled 5 minutes at 100°C, cooled on ice for 5 minutes, centrifuged at 10,000 x g for 5 minutes, and then the protein supernatant loaded into a 12.5 polyacrylamide gel. Proteins were separated on 12.5% polyacrylamide gels at 100V through the stack, and then 200V through the resolving portion of the gel at RT until the dye front ran was no longer visible, about 1hr. Proteins embedded within the gel were transferred to a nitrocellulose membrane for 1hr at 100V at RT and the probed with primary antibodies as per the manufacturer's instructions: mouse polyclonal UCP1 (Abcam, Cambridge, MA), and mouse polyclonal mitofusin-1 (Abcam, Cambridge, MA) were resuspended at 1:1000 in 5% milk in 1X TBST from 1-4 hours at 4°C. The primary antibody for mUCP3 was custom generated for the laboratory by Washington Biotechnology (Columbia, MD) and used at 1:3000 in 5% milk in 1X TBST from 12-16 hours at 4°C. Secondary antibodies were donkey anti-rabbit IgG, (GE Healthcare, UK). Following incubation for 1 hour at RT, membranes were developed using Super Signal West Pico/Femto/Dura chemiluminescent substrate (Pierce, Rockford, IL)

2.8 Immunoprecipitation

Following protein quantification, 250ug of mitochondrial protein lysate was resuspended in 300uL of Hirasaka IP buffer to eliminate non-specific interactions within samples, 1:10 (v/v) of washed Protein A/G Sepharose beads (GE Healthcare, UK**)** were added to samples and allowed to nutate at 4°C for 1 hour. Samples were centrifuged at 10,000 x g for 5 minutes at 4°C and the supernatant transferred to a clean Eppendorf tube. Following this, 2ug of primary

antibody (mUCP1) or IgG control was added to each sample and allowed to rotate end-over-end from 2-4 hours at 4°C. Fresh protein A/G Sepharose beads were thoroughly washed in Hirasaka IP Buffer added at 1:10 (v/v) to samples and were incubated with rotation for at least 4 hours at 4°C. Samples were then centrifuged at 10,000 x g for 5 minutes at 4°C, washed five times with Hirasaka IP buffer, and prepared for immunoblotting via SDS-PAGE as described above.

2.9 Intraperitoneal Temperature Probe Placement

The mouse ventral, right flank was shaved from knee to elbow prior to surgery and mice were placed into an isoflurane-filled chamber until animals no longer exhibited the righting reflex. Once sedated, mice were moved to isoflurane under the nose cone, injected with a pre-operative subcutaneous dose of 1.25mg/kg of Rimadyl (Zoetis Inc., Florham Park, NJ), and the surgical area sterilized using a sterile povidone solution. Utilizing asceptic technique, a small transverse cut was made on the previously shaved flank and the skin spread apart to expose the peritoneum. The same cut was repeated to open the peritoneal cavity and a wireless temperature probe (Starr Life Sciences, Holliston, MA) inserted into the cavity without adhesion to the peritoneal wall. The peritoneal incision was sealed using nonabsorbable vicryl sutures, the skin was closed using sterile skin staples, and mice allowed to recover until fully alert on a heated pad. Twenty-four hours post-op, mice were assessed for signs of infection or duress and given a follow-up subcutaneous dose of 1.25mg/kg of Rimadyl. Mice were allowed to recover for 5-7 additional days prior to experimentation.

2.10 Administration of Thermogenic Agonists

Male mice ages 7-8 weeks were weighed, placed into clean cages containing 70g of bedding with *ad libitum* access to food and water, and placed into a 25°C environment for all temperature studies. Mice were given twenty minutes to acclimate to the 25°C environment prior to recording baseline body temperatures. Subcutaneous injections of either 20mg/kg methamphetamine, or 2mg/kg norepinephrine bitartrate were prepared in sterile saline and injected subcutaneously into the interscapular area, distant from the surgical sites. Body temperatures were recorded using the Vital View software (Starr Life Sciences, Holliston, MA) as per manufacturers directions.

2.11 Statistical Analysis

Statistical evaluation of thermogenic data was performed via IBM SPSS with significance set *a priori* at $p<0.05$. The data represents averages with SEM error bars of at least 3 independent replicates.

Chapter 3 – UCP1 interacts with UCP3 in BAT

Brown adipose tissue is the canonical organ for thermogenesis in small rodents, with UCP1 typically thought of as the key player. However, more research points to UCP3 as a significant auxiliary contributor to UCP1. Studies have shown that UCP3 has the capacity to bind proteins at transmembrane regions as well as N or C-terminal residues (Pierrat *et al.* 2000, Kenaston 2010, Hirasaka *et al.* 2011, Mailloux *et al*. 2011). In addition, it has recently been shown that UCP1 has the capacity to form tetramers with itself (Hoang *et al.* 2013). Thus, it is possible that UCP1 and UCP3 could form oligomers to synergistically augment or facilitate the uncoupling activities of this tissue.

To test whether UCP1 can indeed interact with UCP3 in this tissue, we immunoprecipitated murine UCP1 from WT and UCP3-null BAT lysates and immunoblotted with an antibody against murine UCP3 (**Figure 2**). Following immunoblotting we found a BAT specific interaction between the WT UCP1 and UCP3 that is absent in the UCP3-null samples. However, this immunoprecipitation fails to yield results about the nature of the protein-protein interaction. In this context UCP3 could be directly binding to UCP1 to augment and facilitate the thermogenic response, functioning in an auxillary capacity by exporting LCFA into the mitochondrial matrix to provide an activating substrate for UCP1, functioning in a scaffolding capacity or an effector molecule, mediating ROS generation, or a variety of these functions simultaneously. Further experiments using purified recombinant proteins will uncover the role of UCP3 in this interaction: whether the binding is direct or indirect, and finally, which amino acid residues on both UCP1 and UCP3 mediate this interaction. In addition, the strength of the

interaction can be assessed in the presence of classical UCP activators: treatment with NE, or a combination of oleic and palmitic acids, or thyroid hormone.

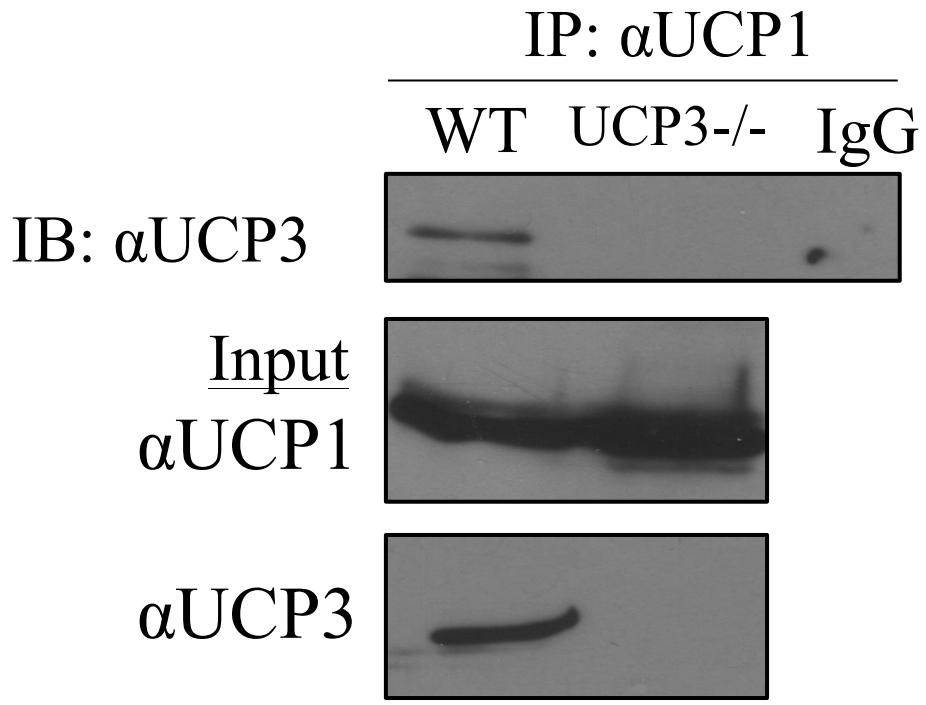

Figure 2. UCP1 interacts with UCP3 in BAT. BAT from WT and UCP3-null mice was excised, processed, and its mitochondrial content purified via density centrifugation. Two hundred and fifty micrograms of mitochondrial lysates were immunoprecipitated with the murine UCP1 antibody or IgG controls and samples prepared for standard 12.5% SDS-PAGE and immunoblotting with αUCP3 antibody.

Chapter 4 – UCP1/UCP3-double null mice exhibit blunted responses to thermogenic challenges

Our current understanding of thermoregulation points to UCP1 as the primary mediator of this mechanism in BAT. However, the role of UCP3 within this tissue is completely unknown. Research from our lab and others has shown that UCP3 has an important and definitive role in mammalian thermogenesis. UCP3-null mice administered MDMA present with a blunted thermogenic response compared to their WT littermates (Mills *et al.* 2003, Sprague *et al.* 2004, 2007). This response has been recapitulated in our lab with the administration of other thermogenic agonists as well, including methamphetamine and lipopolysaccharide (Kenaston 2010). One hypothesis to explain this phenotype postulates that UCP1 and UCP3 interact together additively or synergistically and help mediate the thermogenic response seen upon administration of sympathomimetic agents. This protocol challenged mice with a non-lethal, subcutaneous dose of thermogenic agonists methamphetamine or norepinephrine and monitored changes in body temperature. When methamphetamine reaches the mammalian brain it results in a massive release of norepinephrine throughout the entire body via sympathetic nerve endings (Kish 2008). This also results in the stimulation of the cardiovascular system with concurrent increases in heart hate and blood pressure. Hyperthermia is another common side effect of many stimulating drugs of abuse and hyperthermic responses have been well documented in humans, as well as in many other mammals (Sprague *et al.* 2004, 2005, Levi *et al.* 2012)

This study accomplished two goals: it confirmed results which had been previously generated - that UCP3-null mice fail to mount a hyperthermic response when challenged with

thermogenic agonist methamphetamine, and it provides a first glimpse at the mechanism responsible for this phenotype: a blunted physiological response to norepinephrine (NE).

Twenty minutes after being challenged with a subcutaneous dose of 20mg/kg methamphetamine, all three genotypes reached statistically significant differences in body temperature. Temperature changes peaked at 40 minutes with WT mice having an average increase in body temperature of 1.75 ± 0.11°C (**Figure 3**). This response was significantly blunted in UCP3-null animals who exhibited half the thermogenic response of their WT littermates with raises in body temperature by only 0.75 ± 0.19°C. Most striking, however, is the abolishment of any hyperthermic response in the UCP1/UCP3 double-null animals. These animals actually exhibited a hypothermic response and had a drop in body temperature by -0.87 ± 0.29°C. Furthermore, all three genotypes were able to return their body temperature back to baseline as the methamphetamine was metabolized from their body.

Next, we decided to determine whether the changes in body temperature were definitively due to norepinephrine, or the independent actions of methamphetamine. Indeed, when subcutaneously challenged with 2mg/kg norepinephrine bitartrate, results were very similar to the challenge with methamphetamine only on a slightly earlier timescale. This is explained by the fact that methamphetamine must penetrate the brain before it can exert its actions on the rest of the body. Administration of NE alone does not require this penultimate step and can begin acting on the periphery in less time. In WT and UCP3-null mice changes in body temperature peaked twenty minutes after subcutaneous administration of 2mg/kg norepinephrine bitartrate with an average increase of 0.87 ± 0.15°C and 0.47 ± 0.15°C (**Figure 4)**. Double-null animals exhibited a sharply contrasting hypothermic response, with body temperatures plummeting to -0.34 ± 0.09°C twenty minutes following the thermogenic challenge and reaching

their lowest temperature of -0.50 ± 0.19°C at 60 minutes. Furthermore, unlike all three genotypes in the methamphetamine challenge, UCP1/UCP3 double-null mice failed to bring their body temperatures back to baseline values following the NE challenge – suggesting that UCPs may be involved in returning an organism to homeostatic thermal norms.

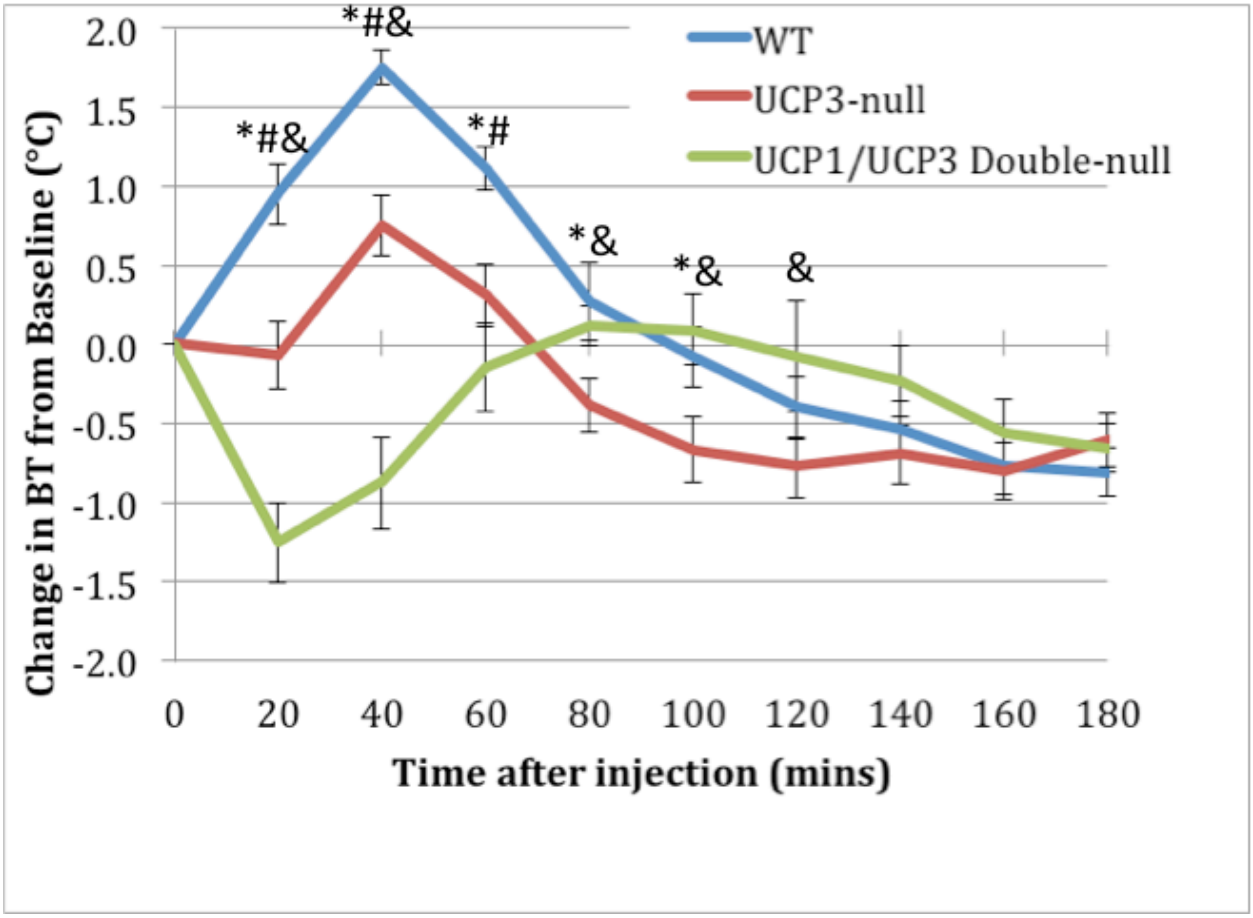

Figure 3. UCP1/UCP3-double null mice exhibit hypothermic responses when challenged with methamphetamine. WT (n=14), UCP3-null (n=10), and UCP1/UCP3-double null (n=6) mice were subcutaneously injected with 20mg/kg methamphetamine and their change in body temperature recorded using telemetry probes. WT mice exhibited the most robust hyperthermic response, followed by UCP3-null mice that had 50% the hyperthermic response of WT mice. UCP1/UCP3 double-null mice showed a greater than 100% hypothermic response compared to WT mice. Data represent averages with error bars representing standard error of the mean (SEM) from at least 3 independent experiments. Statistics were done by an ANOVA followed by a Newmans' post hoc test. * = $p < 0.05$ WT x UCP3-null, # = $p < 0.05$ WT x Double-null, & = $p < 0.05$ UCP3-null x Double-null.

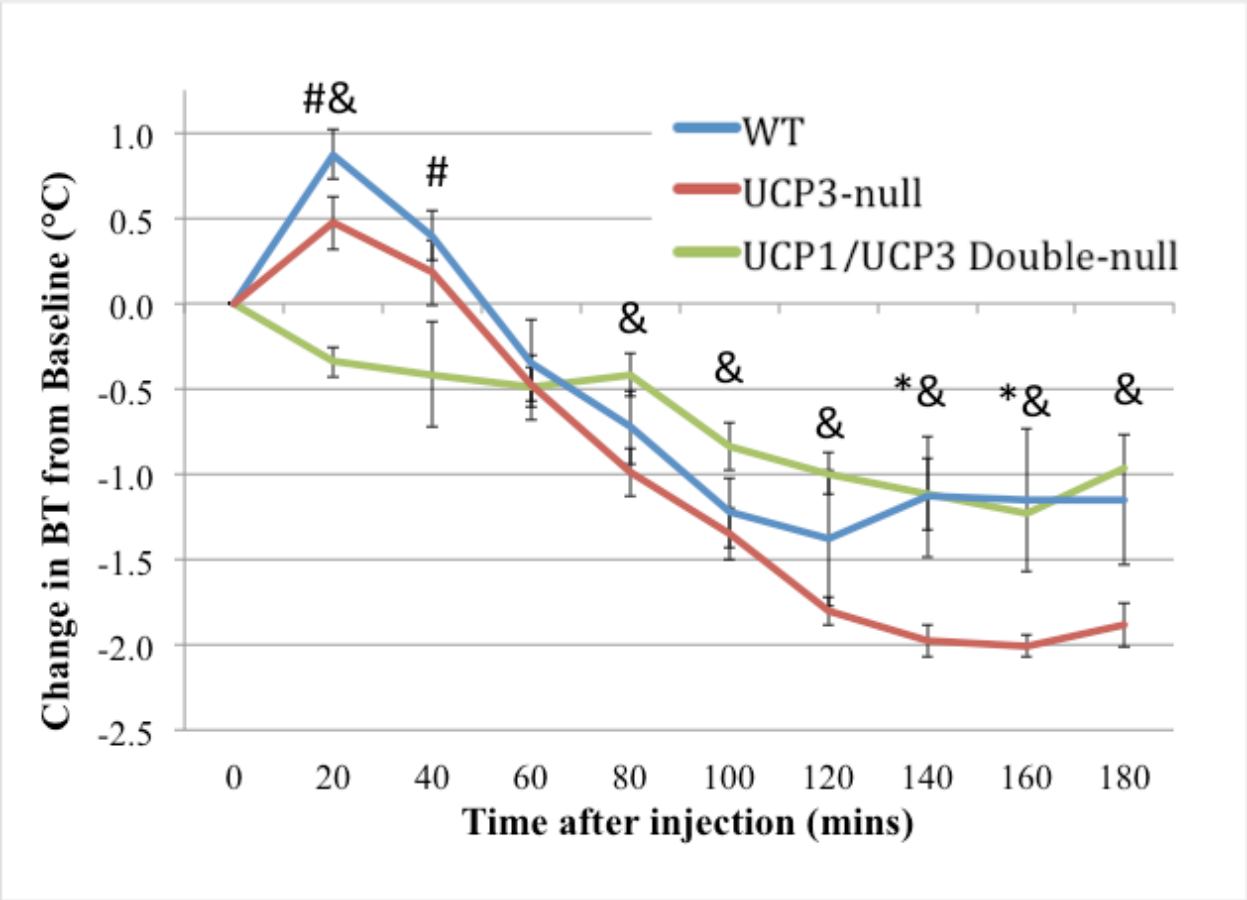

Figure 4. UCP1/UCP3-double null mice have a blunted thermogenic response to NE. WT (n=5), UCP3-null (n=7), and UCP1/UCP3-double null (n=4) mice were subcutaneously injected with 2mg/kg norepinephrine bitartrate and their change in body temperature recorded using telemetry probes. WT mice exhibited the most robust hyperthermic response, followed by UCP3-null mice that had 50% the hyperthermic response of WT mice. UCP1/UCP3 double-null mice showed a 50% hypothermic response compared to WT mice. Data represent averages with error bars representing standard error of the mean (SEM) from at least 3 independent experiments. Statistics were done by an ANOVA followed by a Newmans' post hoc test. * = $p < 0.05$ WT x UCP3-null, # = $p < 0.05$ WT x Double-null, & = $p < 0.05$ UCP3-null x Double-null.

Chapter 5 - Conclusions and Future Directions

Currently, there is no mechanism to explain the hypothermic responses seen in UCP1/UCP3 double-null animals. Following subcutaneous administration of NE, this agonist circulates in the bloodstream before binding to its target receptors around the body. This results in varying effects at differing tissues. In BAT, NE activation results in the initiation of lipolysis – the breakdown of triglycerides into glycerol and the release of FFA. These FFA are then imported into the mitochondria where they are oxidized and can serve as activating substrates for UCPs. Furthermore, activation of the SNS results in increased flux across the ETC and concurrent increases in ROS. Both FFA and various ROS are potent activators of UCPs. With abundant substrates, UCPs can then maximally uncouple respiration from ATP synthesis and generate the most heat possible. Elsewhere in the body, NE acts as a potent vasoconstrictor (Hjemdahl *et al.* 1979). Vasoconstriction keeps warm blood buried deep within the blood vessels and prevents it from heating the periphery – effectively acting as an indirect method of decreasing body temperature. Thus, it is possible that the hypothermia present in UCP1/UCP3 double-null mice has at least two causes: a global lack of UCPs, and peripheral vasoconstriction due to the administration of NE which manifests in the continuous drop in body temperature seen in the UCP1/UCP3 double-null animals. A whole-body lack of UCPs could also help explain the inability of double-null animals to regain their body temperature – as global thermoregulation is compromised by the absence of one or more UCPs.

Our results contrast with the observations made by Gong *et al.* When they challenged UCP3-null mice with β3-adrenoreceptor specific agonist CL316243 they found no change in resting oxygen consumption from WT littermates (Gong *et al.* 2000*)*. Whereas this agonist is

only specific to the β3 group of adrenergic receptors within the murine body, METH and NE both act on all three types of β-adrenergic receptors. Thus, one hypothesis to explain the difference between these results is that murine UCP3 mediated thermogenesis may occur primarily through the β1 and β2 adrenergic receptors in mice. This differs from humans where MDMA-mediated thermogenesis occurs through agonism of the α_1 and the β_3 adrenoreceptors suggesting that these mechanisms vary from one species to the other (Sprague *et al 2004, 2005)*. However, this theory was disproved by Sprague *et al.* By pretreating rats with α_1-adrenergic receptor antagonist, prazosin, and a peripherally selective β_3-adrenergic receptor antagonist, SR59230A, Sprague and his team abolished the MDMA induced hyperthermia and resulting rhabdomyolysis, demonstrating the important, cross-species role mediated by these receptors. (Sprague *et al.* 2004*)*.

We have previously shown that WT mice that have had about 70% of their BAT ablated still present with a hyperthermic phenotype, suggesting the involvement of SKM UCP3 in thermogenesis (Kenaston 2010). Further experiments should be conducted using UCP1/UCP3 double–null mice crossed to UCP3 SKM overexpressing mice, which overexpress human UCP3 in SKM only at levels slightly above the physiological norms. This would shed insight onto whether adding UCP3 back to SKM would be enough to mediate NE-induced thermogenesis, or if this is a phenomenon specifically mediated by the proteins and processes intrinsic to BAT. Lastly, these studies are unfinished, and must be replicated using UCP1-/- mice. Despite trying to breed animals in a variety of temperatures and conditions, UCP1-/- mice failed to produce pups for this study, creating issues in testing a full hypothesis and the interpretation of subsequent results.

Other studies conducted into the function of UCP3 report incongruent results. For example, groups still measure the generation of UCP mRNA following pharmacologic intervention rather than assessing increases in protein levels directly (Margareto *et al* 2001, Mori *et al.* 2004). Messenger RNA in the cytoplasm is incredibly sensitive to degradation by microRNA, short interfering RNA, and endonuclease activity among others. While quantifying mRNA is an easier technique than assessing UCP3 protein content, quantitative PCR only reveals a partial, correlative view of the events occurring in the cell, and must be complimented with a quantitative assessment of UCP proteins, as proteins are the key components within cells which carry out specialized functions. This is made difficult, however, by the dearth of UCP3 in both primary isolated murine BAT cells as well as immortalized BAT cell lines. In addition, following every passage, immortalized adipocytes expressed less and less of UCP1, suggesting that the 3D tissue environment is intrinsic in the maintenance and proper function of UCP1 (unpublished observation).

Classically, many studies assess the function of UCP3 in both BAT and SKM by measuring respiration in isolated mitochondria (Matthias *et al.* 2000, Nabben *et al.* 2011). This often presents confounding results as the removal of an organelle from its natural environment results in the gross perturbation of normal function. These studies also utilize a variety of differing buffers, osmotic media, initial TCA substrates as well as varying levels of important metal cofactors, ADP, and ATP (Ikuma 1970). As a result, the variation in respiration protocols makes it difficult to extrapolate results about UCP3 function in mitochondria. Furthermore, much of what is known about UCP3 has been generated by studying this protein within the context of SKM, where UCP3 is the only UCP present. Groups have published that the redox environment of SKM and BAT varies greatly and could have independent effects on the functions of these

proteins depending on the tissue environment (Mailloux *et al.* 2011, 2012). This makes the study of UCP3 in BAT even more difficult because BAT: a) contains more than one UCP, and b) expresses UCP1 at more than 500 levels greater than UCP3 (Harper *et al.* 2001, 2002). With over 50% amino acid homology, separating the effects of one UCP from another is very difficult. Alternatively, whole-body approaches to assess UCP3 function have presented their own challenges as well. Thermogenic methodologies vary wildly across studies with some groups choosing to acclimate their animals from 4 to 30°C from 1 to 24 hours before challenging them with thermogenic agonists while others do not pre-acclimate. (Feil *et al.* 1994, Cunningham *et al* 2003, Mills *et al* 2003, 2004, Sprague *et al.* 2007).

Previous experiments have assessed UCP3-null FFA oxidation and found no difference between genotypes (Gong *et al.* 2000, Vidal-puig *et al.* 2000). Yet, the majority of theses studies were conducted in SKM and need to be repeated in BAT. Additionally, because our experiments demonstrated UCP3-specific effects following NE administration, future experiments should assess whether NE-stimulated lipolysis is affected by removal of UCP3 in BAT as well as SKM. Furthermore, no studies have assessed whole body plasma FFA and TG levels following NE stimulation in UCP3-null mice. Whole-body ablation of UCP3 could lead to altered lipolytic responses and decreases in circulating FFA. This can be recapitulated *in vitro* by treating differentiated BAT and SKM cells with a variety of thermogenic agonists and then measuring FFA release into the media.

Studies have shown that UCP3-null mice have increased levels of superoxide production in SKM mitochondria (Vidal-puig *et al.* 2000). Furthermore, some groups have discovered that UCP3 has reactive cysteine residues, which have the capacity to modulate ROS generation by the redox cycling of GSH to GSSG (Mailloux RJ, *et al*. 2011, 2012). Thus, future experiments

should assay how UCP3 functions in ROS generation prophylaxis by measuring superoxide production, levels of GSH:GSSG, thioredoxin and aconitase levels in BAT mitochondria of varying genotypes. In addition, elevated ROS has the capacity to damage proteins via carbonylation, and lipid peroxidation. Studies should assess the extent to which UCP3 ablation elevates ROS and its resulting effects on the mitochondrial proteome.

References

Acín A, *et al. Cloning and characterization of the 5' flanking region of the human uncoupling protein 3 (UCP3) gene*. Biochem Biophys Res Commun.258(2):278-83. 1999.

Ali S, *et al. Malignant hyperthermia*. Best Pract Res Clin Anaesthesiol. 2003;17(4):519-33.

Argyropoulos G, Harper ME. *Uncoupling proteins and thermoregulation*. J Appl Physiol. 2002;92(5):2187-98.

Arsenijevic D, *et al*. *Disruption of the uncoupling protein-2 gene in mice reveals a role in immunity and reactive oxygen species production*. Nat Genet. 2000;26(4):435-9.

Bartel D. *et al. Micromanagers of gene expression: The potentially widespread influence of metazoan microRNAs.* Nat. Rev. Genet. 5:396-400. 2004.

Bevilacqua L *et al. Absence of uncoupling protein-3 leads to greater activation of an adenine nucleotide translocase-mediated proton conductance in skeletal muscle mitochondria from calorie restricted mice.* Biochim Biophys Acta. 2010;1797(8):1389-97.

Casteilla, L *et al. Chapter 2: Choosing an Adipose Tissue Depot for Sampling. Factors in Selection and Depot Specificity.* Adipose Tissue Protocols. 2008, XVI, 23-38.

Chelu MG *et al. Heat- and anesthesia-induced malignant hyperthermia in a RyR1 knock-in mouse.* FASEB J. 2006;20(2):329-30.

Criée CP *et al. Body plethysmography--its principles and clinical use.* Respir Med. 2011;105(7):959-71.

Cunningham O, *et al*. *Selective detection of UCP 3 expression in skeletal muscle: effect of thyroid status and temperature acclimation.* Biochim Biophys Acta. 2003;1604(3):170-9.

Dinarello CA *et al. Mechanisms of fever induced by recombinant human interferon.* J Clin Invest. 1984;74(3):906-13.

Echtay KS *et al. Superoxide activates mitochondrial uncoupling proteins.* Nature. 2002;415(6867):96-9.

Enerbäck S. *Human brown adipose tissue*. Cell Metab. 2010;11(4):248-52.

Fedorenko A *et al. Mechanism of fatty-acid-dependent UCP1 uncoupling in brown fat mitochondria.* Cell. 2012; **151**(2):400-13.

Feil S *et al. Effect of acclimation temperature on the concentration of uncoupling protein and GDP binding in rat brown fat mitochondria*. Eur J Biochem. 1994;219(1-2):681-90.

Ferreiro, A. *et al. A recessive form of central core disease, transiently presenting as multi-minicore disease, is associated with a homozygous mutation in the ryanodine receptor \ type 1 gene*. Ann. Neurol. (2002) 51, 750–759

Forner F *et al. Proteome differences between brown and white fat mitochondria reveal specialized metabolic functions*. Cell Metab. 2009;10(4):324-35.

Glazer JL. *Management of heatstroke and heat exhaustion*. Am Fam Physician. 2005;71(11):2133-40.

Gong DW *et al. Lack of obesity and normal response to fasting and thyroid hormone in mice lacking uncoupling protein-3.* J Biol Chem. 2000;275(21):16251-7.

Harms M, *et al. Brown and beige fat: development, function and therapeutic potential.* Nat Med. 2013;19(10):1252-63.

Harper ME *et al. Mitochondrial efficiency: lessons learned from transgenic mice.* Biochim Biophys Acta. 2001;1504(1):159-72.

Harper JA *et al. Artifactual uncoupling by uncoupling protein 3 in yeast mitochondria at the concentrations found in mouse and rat skeletal-muscle mitochondria.* Biochem J. 2002;361:49-56.

Himms-hagen J. *Brown adipose tissue thermogenesis: interdisciplinary studies.* FASEB J. 1990;4(11):2890-8.

Himms-hagen J *et al. Physiological role of UCP3 may be export of fatty acids from mitochondria when fatty acid oxidation predominates: a hypothesis.* Exp Biol Med. 2001;226(2):78-84.

Hjemdahl P *et al. Vascular and metabolic effects of circulating epinephrine and norepinephrine. Concentration-effect study in dogs.* J Clin Invest. 1979;64(5):1221-8.

Hirasaka K *et al. Identification of a redox-modulatory interaction between uncoupling protein 3 and thioredoxin 2 in the mitochondrial intermembrane space.* Antioxid Redox Signal. 2011;15(10):2645-61.

Hoang T *et al. Expression, folding, and proton transport activity of human uncoupling protein-1 (UCP1) in lipid membranes: evidence for associated functional forms*. J Biol Chem. 2013;288(51):36244-58.

Hochaka P *et al. Metabolic Arrest and the Control of Biological Time.* (Pp. 227). Harvard University Press, 1987.

Ikuma H. *Necessary conditions for isolation of tightly coupled higher plant mitochondria.* Plant Physiol. 1970;45(6):773-81.

Jurkat-rott K *et al. Genetics and pathogenesis of malignant hyperthermia.* Muscle Nerve. 2000;23(1):4-17.

Kenaston MA, *et al. Investigation of the Physiological and Biochemical Function of Mitochondrial Uncoupling Protein 3*. Thesis. The University of Texas at Austin. 2010. 1-105.

Kish SJ. *Pharmacologic mechanisms of crystal meth.* CMAJ. 2008;178(13):1679-82.

Kishikawa J, *et al. Molecular basis of ADP inhibition of vacuolar (V)-type ATPase/synthase.* J Biol Chem. 2014;289(1):403-12.

Krauss, S, *et al. "The mitochondrial uncoupling-protein homologues."* Nature Reviews Molecular Cell Biology 6.3 (2005): 248-261.

Levi MS *et al. A comparison of methylphenidate-, amphetamine-, and methamphetamine-induced hyperthermia and neurotoxicity in male Sprague-Dawley rats during the waking (lights off) cycle.* Neurotoxicol Teratol. 2012;34(2):253-62.

Maclellan JD *et al. Physiological increases in uncoupling protein 3 augment fatty acid oxidation and decrease reactive oxygen species production without uncoupling respiration in muscle cells.* Diabetes. 2005;54(8):2343-50.

Mailloux RJ *et al. Glutathionylation acts as a control switch for uncoupling proteins UCP2 and UCP3.* J Biol Chem. 2011;286(24):21865-75.

Mailloux RJ, *et al. Crucial yet divergent roles of mitochondrial redox state in skeletal muscle vs. brown adipose tissue energetics.* FASEB J. 2012;26(1):363-75.

Malte H, *et al. Differential heating and cooling rates in bigeye tuna (Thunnus obesus Lowe): a model of non-steady state heat exchange.* J Exp Biol. 2007;210(Pt 15):2618-26.

Matthias A, *et al. Thermogenic responses in brown fat cells are fully UCP1-dependent. UCP2 or UCP3 do not substitute for UCP1 in adrenergically or fatty scid-induced thermogenesis.* J Biol Chem. 2000;275(33):25073-81.

Mckechnie AE. *Phenotypic flexibility in basal metabolic rate and the changing view of avian physiological diversity: a review*. J Comp Physiol B, Biochem Syst Environ Physiol. 2008;178(3):235-47.

Mills EM, *et al. Pharmacology: uncoupling the agony from ecstasy*. Nature.

2003;426(6965):403-4.

Margareto J, *et al. Changes in UCP mRNA expression levels in brown adipose tissue and skeletal muscle after feeding a high-energy diet and relationships with leptin, glucose and PPARgamma*. J Nutr Biochem. 2001;12(3):130-137.

Martinez-lopez N, *et al. Autophagy in Myf5+ progenitors regulates energy and glucose homeostasis through control of brown fat and skeletal muscle development*. EMBO Rep. 2013;14(9):795-803.

Melin B, *et al. Body temperature and plasma prolactin and norepinephrine relationships during exercise in a warm environment: effect of dehydration.* Eur J Appl Physiol Occup Physiol. 1988;58(1-2):146-51.

Mochizuki K, *et al. Selectivity of fatty acid ligands for PPARalpha which correlates both with binding to cis-element and DNA binding-independent transactivity in Caco-2 cells.* Life Sci. 2006;80(2):140-5.

Mori Y, *et al. Bezafibrate-induced changes over time in the expression of uncoupling protein (UCP) mRNA in the tissues: a study in spontaneously type 2 diabetic rats with visceral obesity*. J Atheroscler Thromb. 2004;11(4):224-31.

Musa CV, *et al. Four novel UCP3 gene variants associated with childhood obesity: effect on fatty acid oxidation and on prevention of triglyceride storage*. Int J Obes (Lond). 2012;36(2):207-17.

Nabben M, *et al. Uncoupled respiration, ROS production, acute lipotoxicity and oxidative damage in isolated skeletal muscle mitochondria from UCP3-ablated mice.* Biochim Biophys Acta. 2011;1807(9):1095-105.

Nabben M, *et al. Significance of uncoupling protein 3 in mitochondrial function upon mid- and long-term dietary high-fat exposure.* FEBS Lett. 2011;585(24):4010-7.

Nedergaard, J. *et al.* (2007) *Unexpected evidence for active brown adipose tissue in adult humans*. *Am. J. Physiol.* 293,E444-E452

Netea MG, *et al. Circulating cytokines as mediators of fever.* Clin Infect Dis. 2000;31 Suppl 5:S178-84.

Pierrat B, *et al. Uncoupling proteins 2 and 3 interact with members of the 14.3.3 family.* Eur J Biochem. 2000;267(9):2680-7.

Ribeiro MO, *et al. Evidence of UCP1-independent regulation of norepinephrine-induced*

thermogenesis in brown fat. Am J Physiol Endocrinol Metab. 2000;279(2):E314-22.

Rosen ED, *et al. Adipocytes as regulators of energy balance and glucose homeostasis. Nature*. 2006;444(7121):847-53.

Rousset S, *et al. The biology of mitochondrial uncoupling proteins.* Diabetes. 2004;53 Suppl 1:S130-5.

Rusyniak D, et al. *The role of mitochondrial uncoupling in 3,4-methylenedioxymethamphetamine-mediated skeletal muscle hyperthermia and rhabdomyolysis.* J Pharmacol Exp Ther. 2005;313(2):629-39.

Saper CB, *et al. The neurologic basis of fever.* N Engl J Med. 1994;330(26):1880-6.

Seale P, et al. *PRDM16 controls a brown fat/skeletal muscle switch*. Nature. 2008;454(7207):961-7.

Shi Y. *Apoptosome assembly*. Meth Enzymol. 2008;442:141-56.

Silva JE. *The multiple contributions of thyroid hormone to heat production.* J Clin Invest. 2001;108(1):35-7.

Solanes G, *et al. Functional relationship between MyoD and peroxisome proliferator-activated receptor-dependent regulatory pathways in the control of the human uncoupling protein-3 gene transcription.* Mol Endocrinol. 2003;17(10):1944-58.

Solanes G, *et al. Thyroid hormones directly activate the expression of the human and mouse uncoupling protein-3 genes through a thyroid response element in the proximal promoter region.* Biochem J. 2005;386 (Pt 3):505-13.

Soumano K *et al. Glucocorticoids Inhibit the transcriptional response of the uncoupling protein-1 gene to adrenergic stimulation in a brown adipose cell line.* Mol Cell Endocrinol. 2000;165(1-2):7-15.

Sprague JE, *et al*. *Attenuation of 3,4-methylenedioxymethamphetamine (MDMA, Ecstasy)-induced rhabdomyolysis with α_1- plus β_3-adrenoreceptor antagonists.* Br J Pharmacol 2004:142 667–670.

Sprague JE, *et al*. *Carvedilol reverses hyperthermia and attenuates rhabdomyolysis induced by 3,4-methylenedioxymethamphetamine (MDMA, Ecstasy) in an animal model.* Crit Care Med 2005:33 1311–1316.

Sprague JE, *et al. Roles of norepinephrine, free Fatty acids, thyroid status, and skeletal*

muscle uncoupling protein 3 expression in sympathomimetic-induced thermogenesis. J Pharmacol Exp Ther. 2007;320(1) 274-80.

Tøien Ø. *Automated open flow respirometry in continuous and long-term measurements: design and principles.* J Appl Physiol. 2013;114(8):1094-107.

Toime LJ, *et al. Uncoupling protein-3 lowers reactive oxygen species production in isolated mitochondria.* Free Radic Biol Med. 2010;49(4):606-11.

Ukkola O, *et al. Genetic variation at the uncoupling protein 1, 2 and 3 loci and the response to long-term overfeeding.* Eur J Clin Nutr. 2001;55(11):1008-15.

Van marken lichtenbelt WD, *et al*. *Cold-activated brown adipose tissue in healthy men.* N Engl J Med. 2009;360(15):1500-8.. 2009; 360(15):1500-8.

Vidal-puig AJ, *et al. Energy metabolism in uncoupling protein 3 gene knockout mice*. J Biol Chem. 2000;275(21):16258-66.

Walder K, *et al. Association between uncoupling protein polymorphisms (UCP2-UCP3) and energy metabolism/obesity in Pima indians.* Hum Mol Genet. 1998;7(9):1431-5.

Wang, Q, *et al. Tracking adipogenesis during white adipose tissue development, expansion and regeneration*. Nat. Med. (2013).